

Discrete-Time Accuracy Analysis of the Time-Domain Regular Perturbation Model for Unamplified Links

Astrid Barreiro*, *Student Member, IEEE* Gabriele Liga*, *Member, IEEE* Tobias Fehenberger† *Member, IEEE*, and Alex Alvarado* *Member, IEEE*

*Eindhoven University of Technology, 5600 MB Eindhoven, The Netherlands

†ADVA, 82152 Martinsried/Munich, Germany

Abstract—The accuracy of a discrete-time channel model based on regular perturbation is numerically studied for unamplified links. We analyse the distance between discrete nonlinear interference points and show that such distance can be used to estimate the effective channel memory.

I. INTRODUCTION

GOOD channel models are key to establish the mathematical framework for a better understanding of nonlinear phenomena and to effectively design fibre-optic communication systems [1]. The nonlinear Schrödinger equation (NLSE), which mathematically describes the propagation of signals in an optical fibre, is the origin for the derivation of most analytical models of nonlinear interference (NLI). In particular, perturbation theory has been broadly employed as the main mathematical method to approximate the NLSE solution and find relatively simplified analytical expressions for the NLI [2], [3].

One of the most popular approximations is based on a regular perturbation (RP) expansion on the nonlinear parameter γ and truncated to the first-order term. Considerable amount of validation work has been carried out on a waveform level [4], [2], [5], [6] for this first-order RP. However, the question of how this accuracy translates to the discrete-time domain has been, to the best of our knowledge, not well addressed in the literature.

In this paper, we numerically study the accuracy of the first-order RP on γ with respect to received symbols observed after chromatic dispersion compensation, matched filtering, and sampling. We consider unamplified links whose study is important for its application to island-to-island communication systems, intra and inter-data center interconnect, and the fact such links are building block for more complex (multi-span) systems.

We assess the convergence of the first-order RP on γ in terms of the model's memory, i.e., on the number of interfering symbols that need to be considered around the symbol of interest to achieve the highest model's accuracy. The model's accuracy is first estimated in terms of predicted NLI variance, a metric often used in the literature. The accuracy of the model is also estimated using the pairwise distance for each

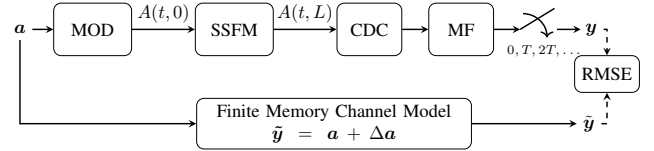


Fig. 1: System model under consideration.

NLI point. This pairwise metric enables a comprehensive assessment of the model's ability to capture the true NLI distribution.

II. SYSTEM MODEL

To assess the accuracy of a perturbative discrete-time channel model, we consider a single channel, single polarization system shown in Fig. 1. The complex transmitted symbols $\mathbf{a} = \dots, a_{-1}, a_0, a_1, \dots$ are converted into an optical field $A(t, 0)$ using linear modulation. Propagation through the optical fiber is performed via the split step Fourier method (SSFM), which we consider the true channel. At the receiver, chromatic dispersion compensation (CDC) is applied to the received field $A(t, L)$. Matched filter and sampling at the symbol rate is used to obtain the vector of symbols $\mathbf{y} = \dots, y_{-1}, y_0, y_1, \dots$, where y_0 represents the received symbol at time instant 0.

The first-order RP on the nonlinear parameter γ approximates the exact solution of the NLSE and leads to a discrete-time channel model given by $\tilde{y}_0 \approx y_0$, where

$$\tilde{y}_0 \approx a_0 + \Delta a_0, \quad (1)$$

with

$$\Delta a_0 = j\gamma G \sum_{k_1=-N}^N \sum_{k_2=-N}^N \sum_{k_3=-N}^N a_{k_1}^* a_{k_2} a_{k_3} \mathcal{S}_{k_1, k_2, k_3} \quad (2)$$

and where k_1, k_2, k_3 are time indices, and $\mathcal{S}_{k_1, k_2, k_3}$ are complex coefficients that model self-phase modulation [6]. In (2), G is a scaling factor to control the transmit power P . As shown in (2), we focus on a finite memory model, which converges to the first order perturbative model when $N \rightarrow \infty$. The value of N is referred as the *model memory*, where $2N + 1$ is the number of interfering symbols.

The methodology we propose to evaluate the accuracy of the model is shown in Fig. 1. The channel model in (2) is

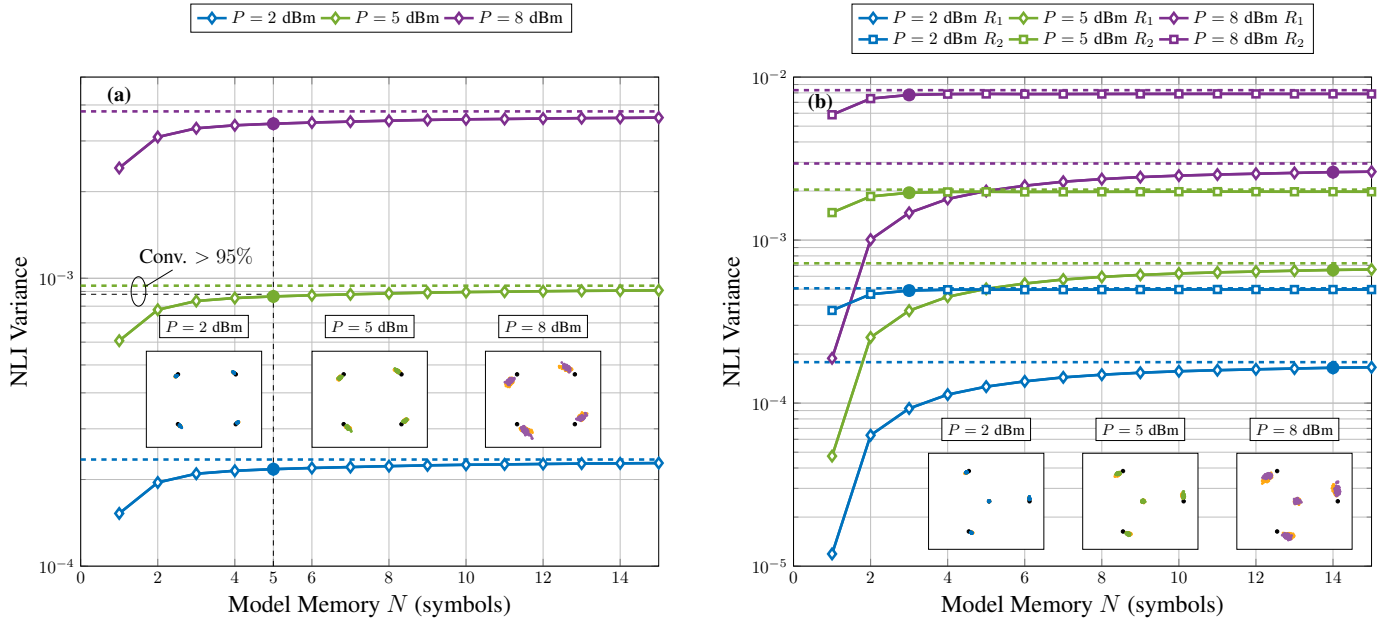


Fig. 2: NLI variance vs. model memory N for QPSK (a) and 1-3-APSK (b). The filled markers represent the model memory estimated via the NLI variance of the RP model on γ .

TABLE I: Fiber parameters

Nonlinearity parameter γ	$1.2 \text{ W}^{-1}\text{km}^{-1}$
Fiber attenuation α	0.2 dB/km
Group velocity dispersion β_2	$-21.7 \text{ ps}^2/\text{km}$

used as a parallel response function that based on the channel input \mathbf{a} , estimates symbol-by-symbol the real channel output \mathbf{y} . The vectors \mathbf{y} and $\tilde{\mathbf{y}}$ are used to compute the NLI variances $\text{Var}[Y_0 - A_0]$ and $\text{Var}[\tilde{Y}_0 - A_0] = \text{Var}[\Delta A_0]$, which follows from (1) and (2).

In addition, we propose to study the random variable

$$W(\mathbf{a}) \triangleq |Y_0(\mathbf{a}) - \tilde{Y}_0(\mathbf{a})|, \quad (3)$$

where the dependency on the transmitted symbol sequence \mathbf{a} is made explicit to emphasize that Y_0 and \tilde{Y}_0 are obtained using the exact transmitted sequence \mathbf{a} . In the next section we study the distribution of the random variable $W(\mathbf{a})$ as well as its root mean square error.

III. NUMERICAL RESULTS

The system under study is a 32 Gbaud single-channel transmission with root-raised cosine pulse shaping (10% roll-off) over a single span of standard single-mode fiber, with parameters summarized in Table I.

Fig. 2(a) shows the NLI variances for $L = 200$ km as a function of the model's memory size N for three different transmitted powers ($P = 2, 5, 8$ dBm, with $P = 5$ dBm being optimum launch power) and for a quaternary phase shift keying (QPSK) modulation format. We observe that the variance predicted by the model in (1)–(2) saturates at $N = 5$ symbols for all transmitted powers (considering a convergence $> 95\%$ of the asymptotic variance value). This indicates no significant power dependence of the channel memory in the

considered power interval, which combines both linear and low non-linear regimes. The variance predicted by the model for large values of N converges to the variance estimated using SSFM simulations (dashed lines). In Fig. 2(b), the NLI variance is analysed for a 1-3 amplitude-phase shift keying (APSK) format on a per-ring basis and for the three above mentioned transmitted powers. In 1-3-APSK, one point is at the origin (i.e., the first ring $R_1 = 0$) and the other 3 points are equally spaced on a ring R_2 . Fig. 2(b) shows that the model predicts well different values of the variance for the two constellation rings, where the variance of R_1 is considerably lower than the variance for R_2 . This is particularly evident from the insets in Fig. 2(a), specially for $P = 8$ dBm. Moreover, the saturation of the variance for the two rings is achieved at different memory values (see filled circles). These results indicate that the channel memory (in a NLI variance sense) is input-dependent.

To extend the picture given by the NLI variance, we analyse the random variable in (3). In particular, we study the mean value, which corresponds to the root mean squared error (RMSE) between the received symbols in (1) and the corresponding SSFM estimates, i.e., $\text{RMSE} = E[W]$. The RMSE is able to capture the proximity between the NLI deviations predicted by the model and the corresponding values obtained via the SSFM, thus providing a more comprehensive picture of the model's convergence to the true NLI distribution. Fig. 3 shows the RMSE as a function of the model's memory N , for QPSK (a) and 1-3 APSK (b). Fig. 3(a) shows that for all powers the RMSE saturates at a value of $N = 5$, confirming the results obtained via a variance-based memory estimation. This is also confirmed by the histograms of W (insets in Fig. 3) which are similar for all powers (up to a rescaling of their x -axis). The asymptotic RMSE decreases as the transmitted power is decreased, which indicates that the

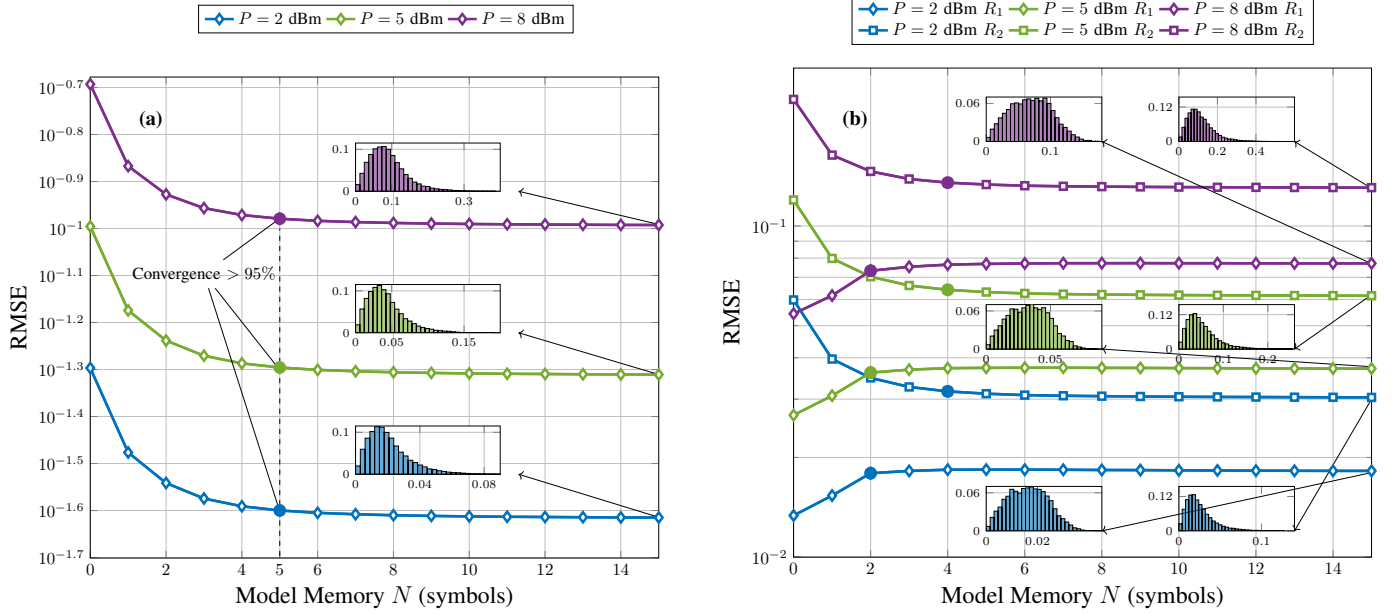


Fig. 3: RMSE vs. model memory N for QPSK (a) and 1-3-APSK (b). The insets show the histograms of W in (3). The filled markers represent the model memory estimated via the NLI variance of the RP model on γ .

model's accuracy is limited by the second and higher order terms of the perturbation expansion.

On the other hand, the APSK results shown in Fig. 3(b) demonstrate a dependency of the model's convergence on the specific ring we constrain our input symbol on. Both the value of N at which the RMSE reaches convergence (shown with filled markers) and the asymptotic RMSE value are ring-dependent. Moreover, for a given ring the value of N at which the RMSE reaches convergence is power independent. Specifically, it can be seen that for the inner ring the model's memory is given by $N = 2$, while for the outer ring the memory is $N = 4$. This input dependence of the RMSE is due to the mathematical form of (1) which shows how the NLI arises from a coherent combination of the complex coefficients $\mathcal{S}_{k_1, k_2, k_3}$ and the specific set of triplets weighing these coefficients. As the symbol of interest is constrained to a given ring of the APSK constellation, each kernel is weighted by a specific subset of possible triplets. Such subset, together with the structure of kernel set determines the model's convergence as a function of N , and as a result the channel memory. The variation of the memory as a function of the constellation ring is also demonstrated by the histograms in Fig. 3(b) which are shown for $N = 15$ and for the two different APSK rings. Indeed, for each power the distributions of the NLI distances W are considerably different for the two rings examined and each ring-constrained distribution is approximately invariant to transmitted power.

IV. CONCLUSIONS

We presented a study of the accuracy of a well-established time-domain RP model based on the comparison between the discrete NLI obtained using SSFM simulations and the one predicted by the model itself. Through this comparison we characterised the channel memory of a single-span optical fiber

system. We found that both in terms of NLI variance and RMSE the RP model shows a good convergence to SSFM results using a truncation window or *model memory* of about $N = 5$ for a QPSK modulation format. For the 1-3 APSK format, the value of N at which the model converges to the true NLI is ring-dependent. Future work includes a memory analysis of multi-span multi-channel systems.

ACKNOWLEDGMENTS

The work of A. Barreiro and A. Alvarado has received funding from the European Research Council (ERC) under the European Union's Horizon 2020 research and innovation programme (grant agreement No 757791). The work of G. Liga is funded by the EuroTechPostdoc programme under the European Union's Horizon 2020 research and innovation programme (Marie Skłodowska-Curie grant agreement No. 754462).

REFERENCES

- [1] A. Bononi, R. Dar, M. Secondini, P. Serena, and P. Poggiolini, "Fiber Nonlinearity and Optical System Performance," 2020, pp. 287–351. [Online]. Available: http://link.springer.com/10.1007/978-3-030-16250-4_{_}9
- [2] A. Vannucci, P. Serena, and A. Bononi, "The RP method: A new tool for the iterative solution of the linear Schrödinger equation," *Journal of Lightwave Technology*, 2002.
- [3] E. Forestieri and M. Secondini, "Solving the nonlinear Schrödinger equation," *Optical Communication Theory and Techniques*, no. 1, pp. 3–11, 2005.
- [4] V. Oliari, E. Agrell, and A. Alvarado, "Regular perturbation on the group-velocity dispersion parameter for nonlinear fibre-optical communications," *Nature Communications*, vol. 11, no. 1, pp. 1–11, 2020. [Online]. Available: <http://dx.doi.org/10.1038/s41467-020-14503-w>
- [5] M. Secondini and E. Forestieri, "Analytical fiber-optic channel model in the presence of cross-phase modulation," *IEEE Photonics Technology Letters*, vol. 24, no. 22, pp. 2016–2019, 2012.
- [6] R. Dar, M. Feder, A. Mecozzi, and M. Shtaif, "Properties of nonlinear noise in long, dispersion-uncompensated fiber links," *Opt. Express*, vol. 21, no. 22, pp. 25 685–25 699, nov 2013.